Ray-level deep-learning-based correction for enhanced universal flux density predictions SolarPACES 2025

Sergio Díaz Alonso*1, Christian Raeder1, Bernhard Hoffschmidt2,

¹Deutsches Zentrum für Luft- und Raumfahrt (DLR), Institute für Solar Forschung, Jülich, Germany ²,RWTH Aachen University, Aachen, Germany

*sergio.diazalonso@dlr.de

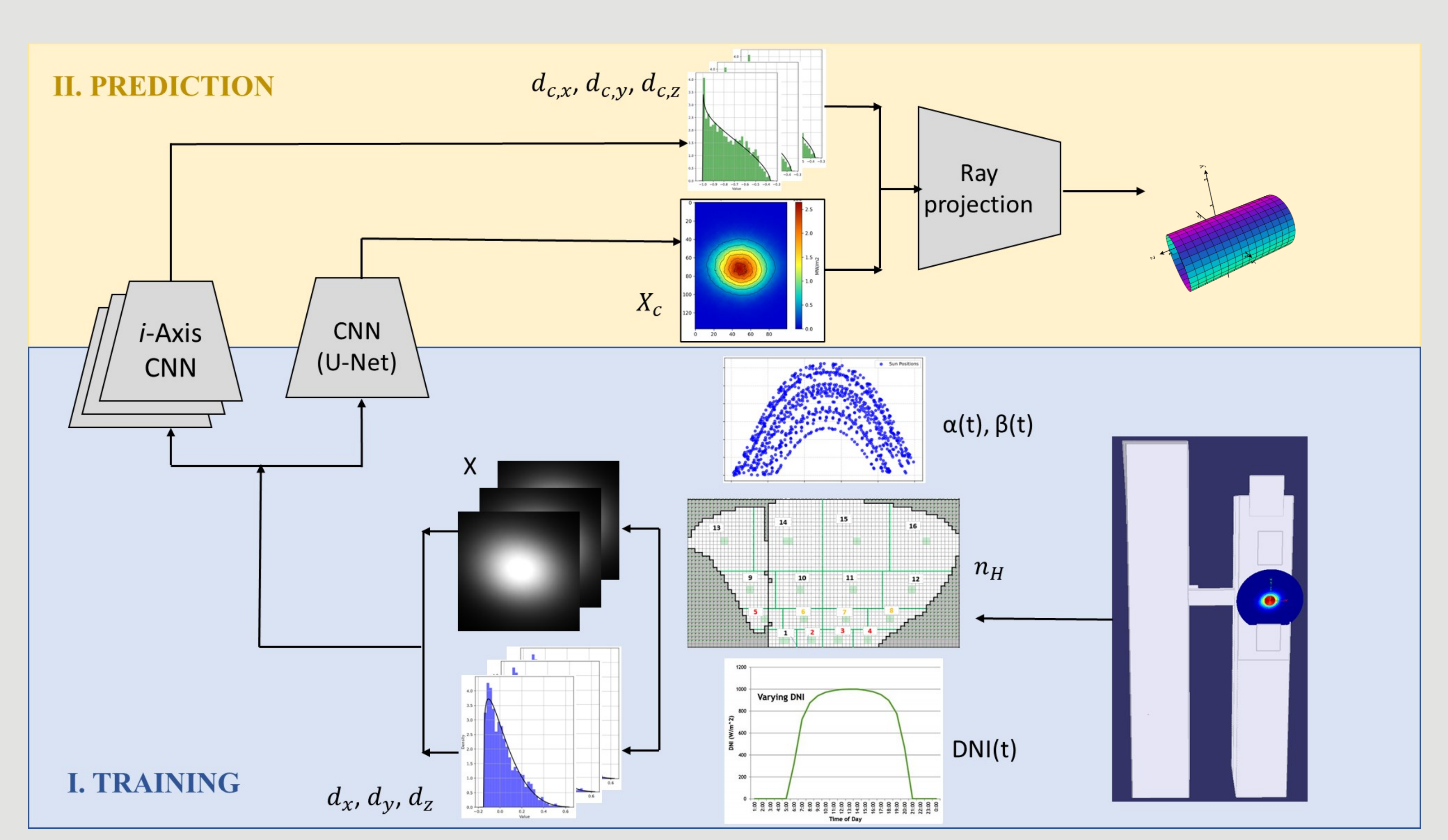


Fig. 1. Complete operation flow diagram. Several thousands of flux maps (X) and simulated ray files (d_x , d_y , d_z) are obtained at the receiver aperture plane from the simulation environment at Sim2Sim step. The neural networks then predict realistic fluxes at the aperure plane from ideal cases and the rays are projected towards 3D surfaces.

1. Introduction

Concentrating Solar Technologies (CST) arise as a significant option in the energy transition towards European Union net-zero greenhouse gas emissions target by year 2050. They are able to participate in electric power generation, in green fuels synthesis, and in industrial heat generation. Among the different CST layouts, the future research trends aim to Solar Power Tower (SPT) systems, due to their ability to reach high operational fluxes and temperatures. However, these systems still require to increase their optical and thermal efficiences, to improve dispatchability and flexibility, to reduce operation and maintenance costs, and to ensure reliability.

In this concern, flux density prediction is one of the most important on-duty procedures, in order to quantify receiver efficiency, as well as other important operating conditions, like incident flux distribution smoothness. Most of the state-of-the-art methods are based on ray-tracing simulations and camera-based procedures. The authors acknowledge each of these methodologies' strengths and propose a hybrid and universal datadriven flux prediction methodology, combining and leveraging cameras and simulations, while trying to avoid their inconveniences. The main design requirements are reduced costs, near-real-time result obtention, continuous and non-disruptive operation, accuracy, and universality.

This methodology consists on the usage of 4 different neural networks (CNNs) to provide the models with realistic features. As seen in Fig. 1, a neural network is used to provide superposed ideal simulated flux maps (without tracking error models) with direction and power features from realistic simulations in first instance (Sim2Sim), and experimental measurements later (Sim2Real). Those realistic features are provided through systematic comparison between simulations and camera-based flux density measurements at the receiver aperture plane, as shown in Fig. 2. The images can be obtained out of working hours (during construction, for example) and optical cameras and targets can be dismantled for normal operation, what allows a consistent O&M cost reduction.

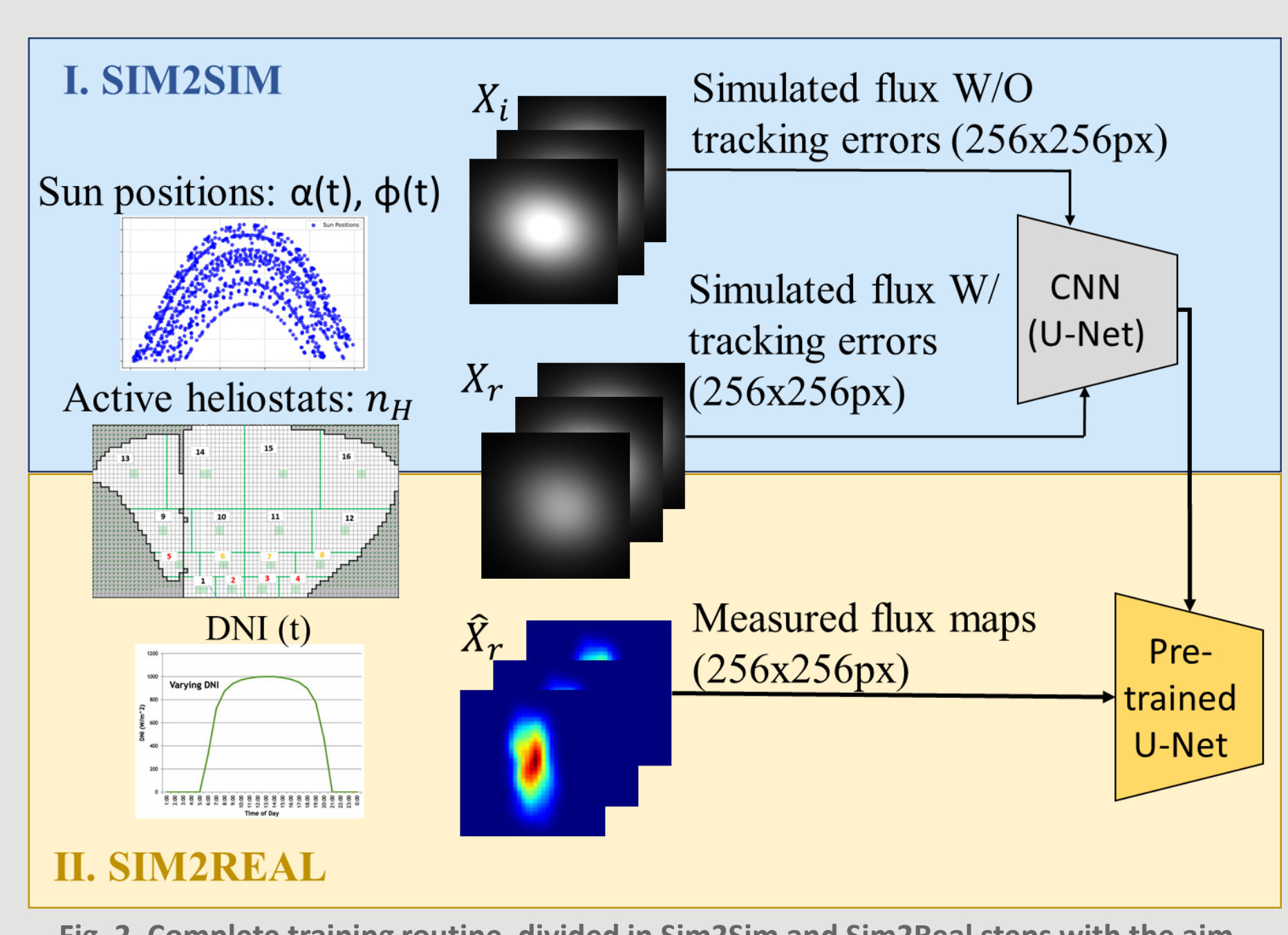


Fig. 2. Complete training routine, divided in Sim2Sim and Sim2Real steps with the aim to address the parametric complexity.

2. Ray-level power correction

The ray-level power correction leverages an attention-gated and tuned U-Net approach, specifically tailored for continuous distribution replications. Its input is a 1-channel 256x256 px picture that gets downsampled 5 times through succesive convolutional filters in order to extract the most relevant features and then reconstructed through the 5 upsampling layers to recover the original size. This neural network has been trained on a dataset composed of 15927 simulated pairs of flux maps, based on realistic experimental conditions collected between 2014 and 2016 at Solartrum Jülich (STJ) [1]. The 15928 inputs are simulated without tracking errors and the groundtruths are simulated with them.

Then, the input (ideal) and the prediction (realistic) are downsampled to a 13x13 elements grid. Each of this grid's values are the averages of each element pixels. These values are then divided in order to get the average power gain factor and the simulated ray power is multiplied times the gain factor that correspond to the element where they intercept the aperture plane. The process is summarised in fig. 4.

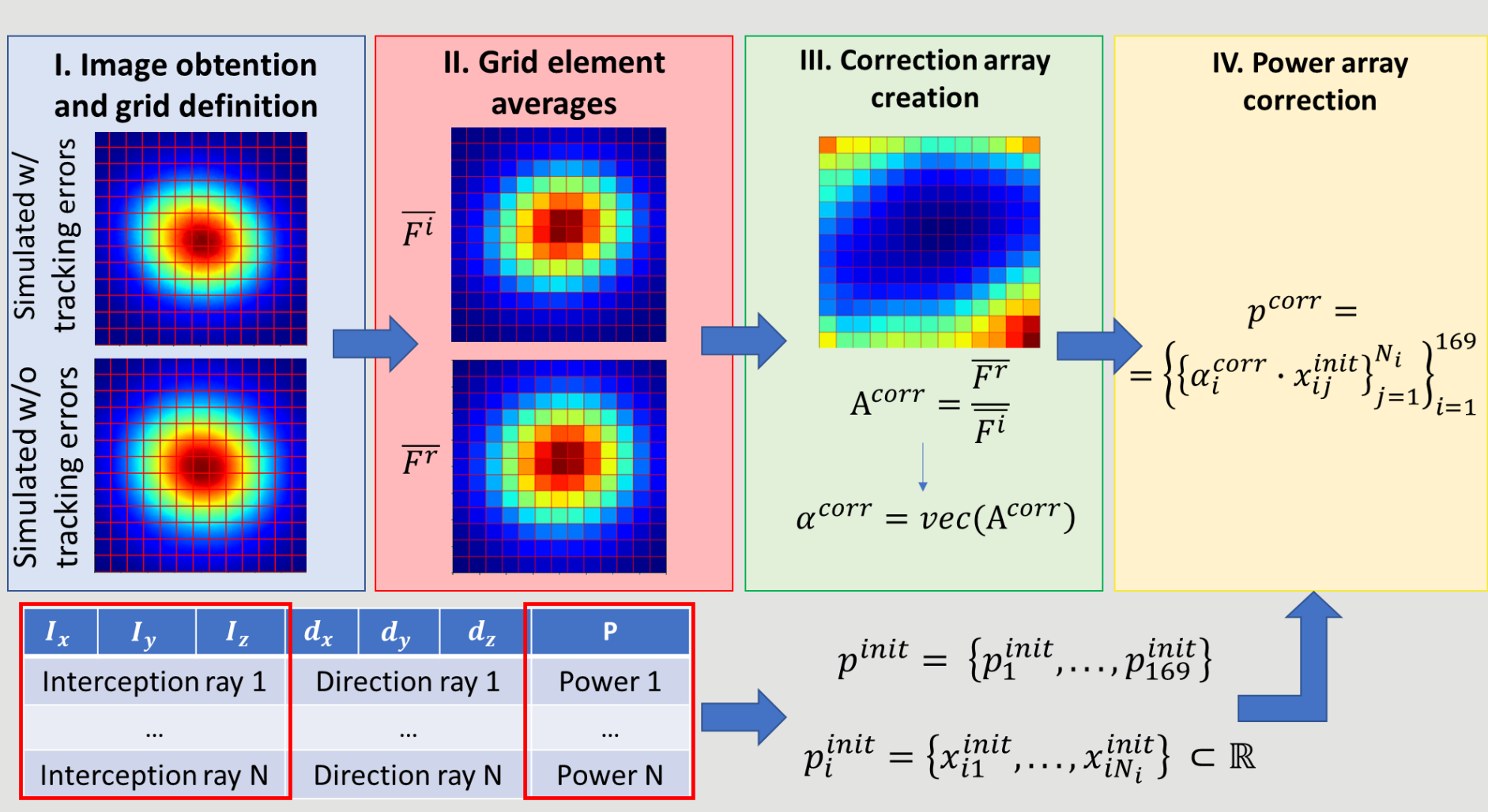


Fig. 3. Power correction procedure.

The image corrections (for flat surfaces) have been tested at 9 DNIs between 100 W/m² and 900 W/m², and at 7 different sun positions. The average accuracy has been 88% (95% CI [87, 89]%) with robust performances around 90% for DNIs ranging from 500 to 900 W/m² (usual operation conditions) and higher sun positions. The highest flux prediction errors are below 8%.

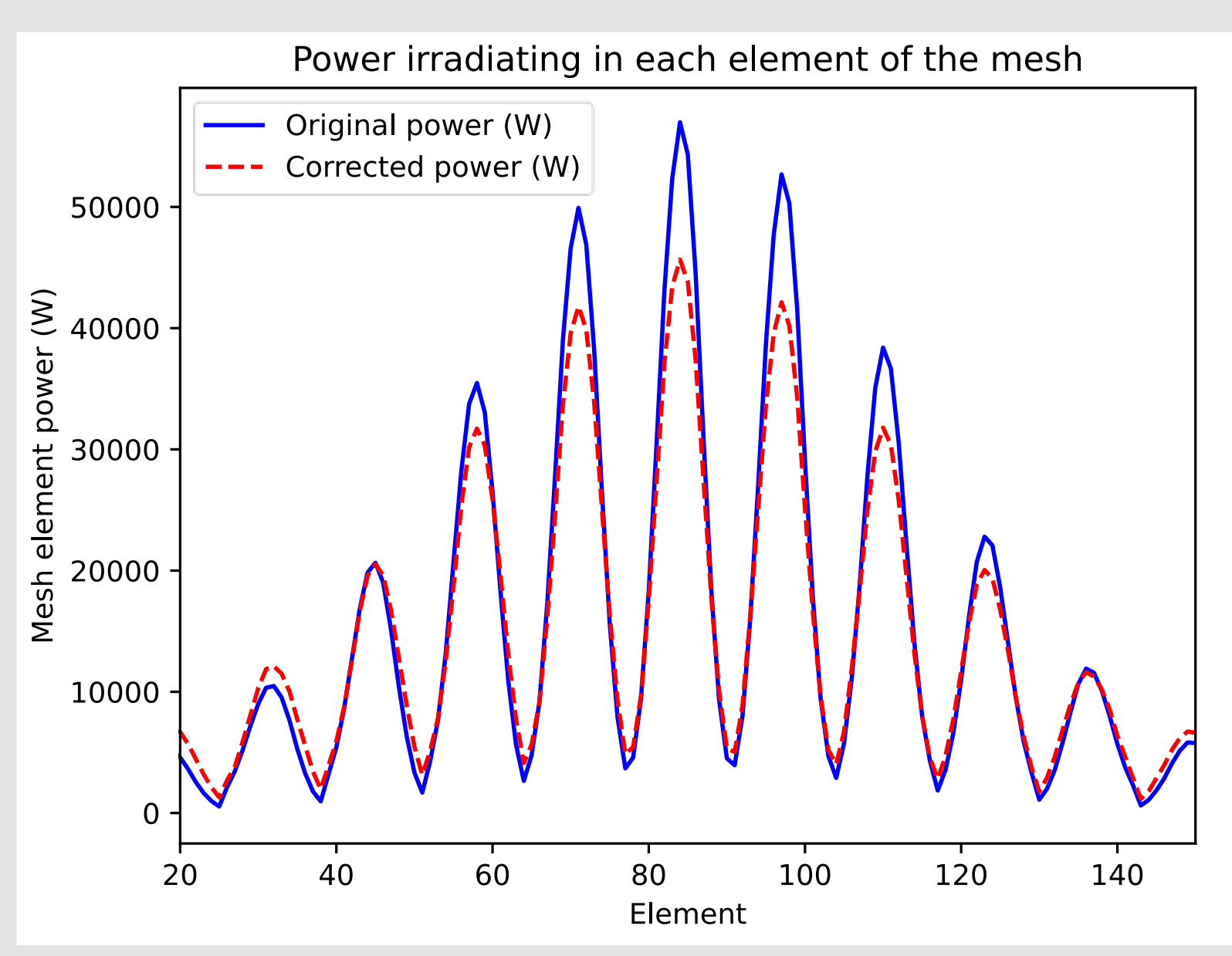


Fig. 3. Power correction per element at 900 W/m² the 01-08-2022 at 15:00:00

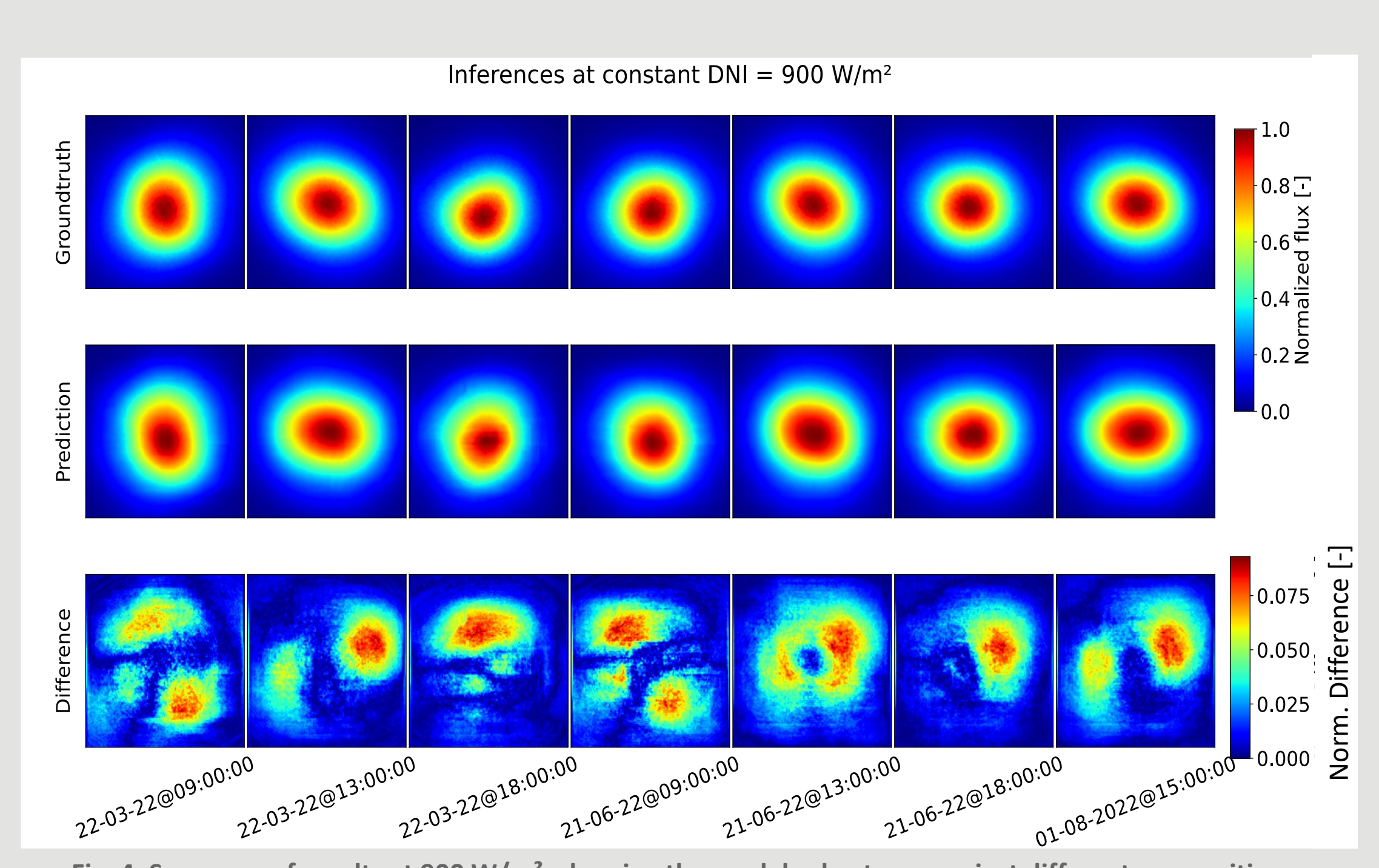


Fig. 4. Summary of results at 900 W/m², showing the model robustness against different sun positions.

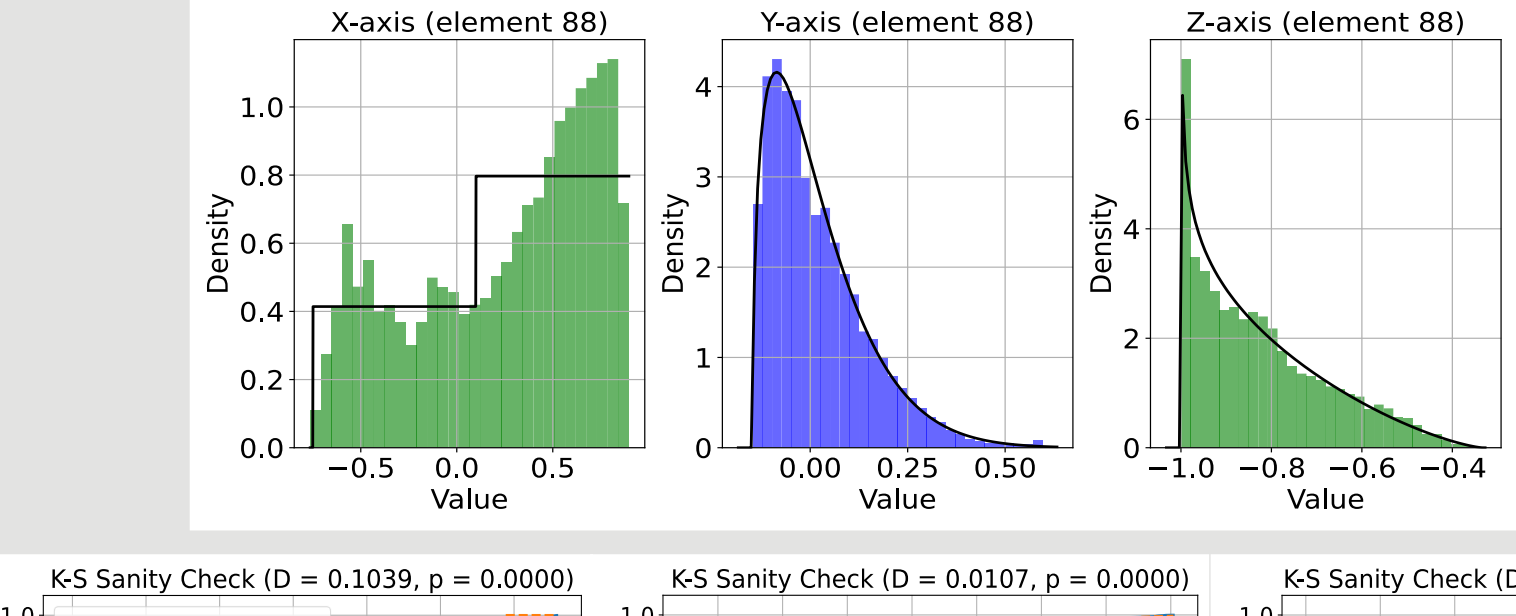
3. Ray-level direction correction

In this case, the dimensional complexity needs to be reduced a second time: after the image is downsampled and the rays are classified along the 169 elements, their directions are fitted to 3 probability density functions (PDF) element-wise. In X-axis, the distribution is a double-step function (eq. (1)), and in Y and Z-axis, it is a Beta distribution function (eq. (2)).

$$f_{x}(x) \begin{cases} 0 & if \ x < x_{1} \\ a_{1} & if \ x_{1} < x < x_{2} \\ a_{2} & if \ x > x_{2} \end{cases}$$
 (1)

$$f_{y}(x;\alpha,\beta,a,s) = \frac{1}{s \cdot B(\alpha,\beta)} \left(\frac{x-a}{s}\right)^{\alpha-1} \cdot \left(1 - \frac{x-a}{s}\right)^{\beta-1} \sim f_{z}(x;\alpha,\beta,a,s)$$

Where α , β > 0 are the shape parameters and B(α , β) is the standard beta distribution function.



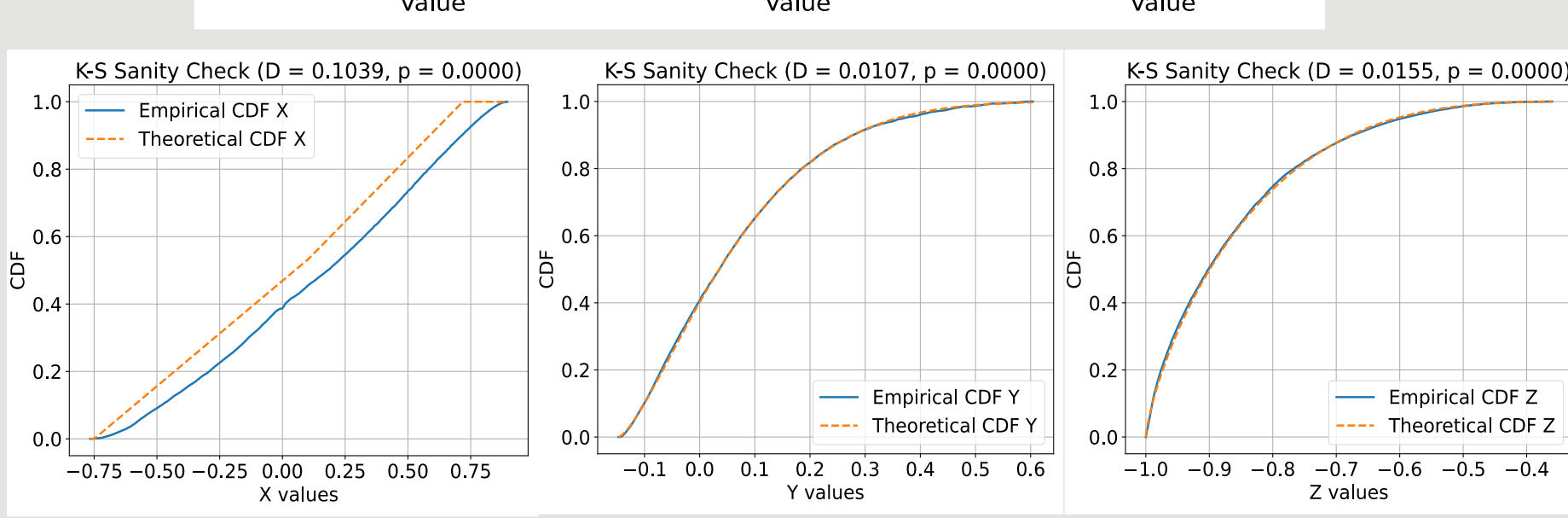


Fig. 4. Element 85 axis-wise distribution fitting (above) and Kolmogorov-Smirnov sanity check for 13-05-2022 at 11:30.

According to Fig. 4, the fittings reveal maximum deviations of 10.39% for X-axis and down to 1-2% for Y and Z-axes in central grid elements. For peripheral elements, these values reach 15% in Xaxis and 2-3% in Y and Z-axes.

The 4 parameters of each distribution are then corrected in a CNN trained on realistic simulations (with tracking errors). The result is a set of 169 realistic direction distributions. From there, the algorithm generates pseudo-random rays, governed by the corrected distributions element-wise.

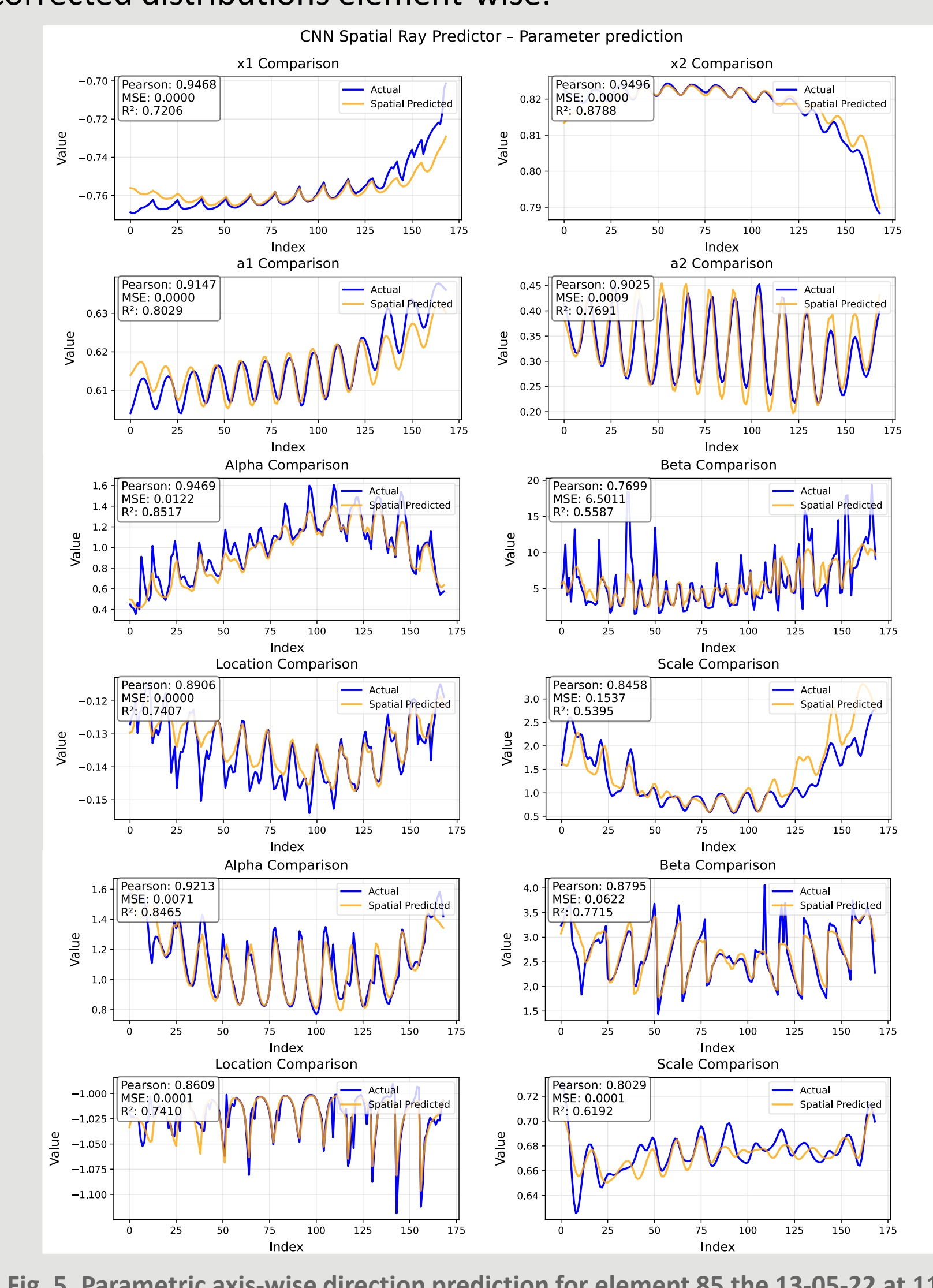


Fig. 5. Parametric axis-wise direction prediction for element 85 the 13-05-22 at 11:30

project has been funded by European Union Horizon 2020 MSCA. agreement Project number grant 101072537.





